International Journal of Advanced Engineering Research and Science (IJAERS)
Peer-Reviewed Journal
ISSN: 2349-6495(P) | 2456-1908(O)
Vol-9, Issue-12; Dec, 2022
Journal Home Page Available: https://ijaers.com/
Article DOI: https://dx.doi.org/10.22161/ijaers.912.20

Development of a low-cost microclimate monitoring system through IoT, using long-range technology (LoRa)

R. Camparim[1], M. E. Petenuci[2], Y. R. Súarez[3]

[1]Faculty of Engineering of the Universidade Federal da Grande Dourados, Dourados, Mato Grosso do Sul, Brazil
[2]State University of Mato Grosso do Sul, Dourados, Mato Grosso do Sul, Brazil
[3]Natural Resources Program, State University of Mato Grosso do Sul, Dourados, Mato Grosso do Sul, Brazil

Received: 16 Nov 2022,

Receive in revised form: 08 Dec 2022,

Accepted: 13 Dec 2022,

Available online: 19 Dec 2022

***Keywords*— Microprocessed Systems, Internet of Things, LoRa, Remote Monitoring, Microclimatic.**

***Abstract*—*The Internet of Things (IoT) can be a means of inserting the environment into our daily lives. IoT allows remote monitoring of any area or process, providing greater reliability. Therefore, this work aimed to develop a low-cost microclimate monitoring system through IoT, using long-range (LoRa) technology with radiofrequency communication between the receiver and the transmitter systems. Two WiFi LoRa 32 V2 modules were used to develop data acquisition systems with independent information storage. For microclimate monitoring, temperature sensors, relative air humidity, illuminance, anemometer and a MicroSD card module were used, connected to the data acquisition transmitter system (DAQ_T). This system was packaged into polyvinyl chloride (PVC) tubes for outdoor protection. The modules were programmed through the Arduino IDE (Integrated Development Environment) platform, which permits the development of a web service for real-time data visualization and, as support for monitoring and data storage by the ThingView App. All sensors were tested and compared with reference equipment to ensure its effectiveness and efficiency. After numerous tests, the developed system presented satisfactory results and reached 3.5 km of intermittent communication between receiver and transmitter of the develop system. Consequently, this system could be considered a low-cost option to be applied in microclimate monitoring or environmental monitoring, including places without internet network.*

I. INTRODUCTION

The current economic development model is based on the industrial format, which uses natural resources in an unsustainable form, impacting the environment and compressing human life [23]. The main effect of these interferences is related to climate change, mainly the increase of global temperature due to the concentration of carbon dioxide (CO2), methane (CH4) and nitrous oxide (N2O). Thus, the effect of these impacts on the ecosystem directly affects environmental systems, human health, agriculture, food, hydrological cycles, increasing the frequency and intensity of droughts and floods and causing redistribution of water resources [22].

The essence of sustainable development emerged in the 1980s, aiming to combine economic and social growth with environmental preservation and more efficient management of natural resources. The World Commission on Environment and Development has defined the concept of sustainable development as "a development that meets the needs of the present without compromising the ability of future generations to meet their own needs". So, this concept considers that, while development is imperative to meet the needs of society and improve the quality of life, it

must be in a way that it does not compromize the capacity of the natural environment to meet present and future needs [30].

The environment protection is a principle of economic order and it is also provided in the Brazilian Constitution, which seeks to harmonize economic activity with environmental preservation [5]. Recently, economic growth is being combined with environmental preservation by integrating the environment with current technology, through the Internet of Things (IoT).

According to [13], IoT is defined as a network infrastructure at a global level, which allows interaction with objects that are interconnected by the Internet. The IoT application in the environment makes it more technological with the use of sensors, antennas, microcontrollers, automation systems, monitoring and data acquisition systems, controlling systems and other electronic components. So, all the data collected by these electronic components could be named as Data Acquisition System, such as DAQ or DAS. References [7]-[10], defined these systems as responsible for the measurements of physical phenomena (signals) and recorded it for further analyses. A signal can be a combination of one or more independent variables and its alternation evidences some physical phenomenon. Through digital electronics, signals can be divided into branches, the most common being the analog signal processing; the other is the digital signal processing, resulting from the combination of adapted analog techniques with other inherently digital techniques [6]. Therefore, the signals obtained by the DAQ are converted from the analog domain to the digital domain and then recorded in a digital medium.

Generally, current digital data acquisition systems are composed by four essential components: sensors, signal conditioners, analog-to-digital converters and computer with DAQ software for recording and analysis [8]. According to [18], in the IoT, the receiver and the sender are things or objects that use the internet as a means of communication and interaction. Thus, many researchers show the integration of those low-cost data acquisition equipment in environmental monitoring [4]-[12]-[32]. However, these studies do not show the validation of the sensors used, that is, they do not demonstrate the efficiency of the sensors for the proposed application.

Therefore, considering that actions must be faster in relation to environmental degradation, as well as the financial cost to make this connection, this work aims to develop a data acquisition system (DAQ) and a low-cost communication system to connect the environment and the technological world through a peer-to-peer communication system with LoRa (Long Range) network.

II. MATERIALS AND METHODS

The low-cost DAQ system structure proposed in this study for long-range microclimate monitoring is composed of sensors, battery and two microprocessor boards; one acting as a receiver and the other as a transmitter with RFID (Radio Frequency IDentification) communication between it. According to [28], RFID is a technology for identifying, objects tracking and data submission, using radio waves as a mean of communication to transfer information.

Sensors of DAQ system are responsible for the microclimate monitoring parameters: temperature, humidity, illuminance, wind speed and battery voltage level. All information is processed and stored by this system.

1. IoT board

The IoT-based development board used was the WiFi LoRa 32 V2, which is a long-range IoT produced by Heltec Automation (TM. This board is equipped with ESP32 WiFi, Bluetooth Low Energy and the Tensilica LX6 Dual Core processor operating at up to 240Mhz, working alongside LoRa SX1276 transceiver, 0.96-inch 128x64 OLED display, and it is still equipped with lithium battery charging and discharge circuit. The SX1276 chip is the Remote LoRa modem™ 915 MHz frequency, about -148dBm high sensitivity, power output of +20 dBm, responsible for communicating and sending data packets between the boards [15].

2. Transmitter system and data recorder

Data recorder is used to register data from sensors or external instruments over time, storing this data on a MicroSD card [20]. The transmitting system is responsible for collecting data and sending packages with all microclimate information. This system is called DAS_T (Transmitter Data Acquisition System). The DAS_T architecture is illustrated in Fig. 1.

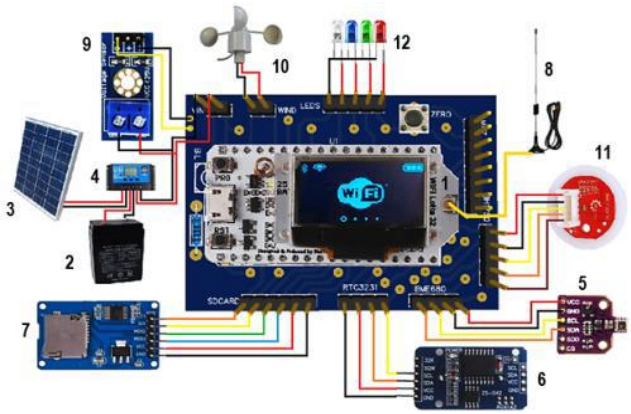

Fig. 1 DAS_T system structure. (1) LoRa 32 V2 WiFi board; (2) Rechargeable 12v 5Ah Battery; (3) Photovoltaic solar plate PANEL KOMAES Km 10w; (4) Load controller model PWM10A; (5) BME680 sensor of temperature, humidity, pressure and altitude; (6) Real-time clock module RTC Ds3231; (7) MicroSD module card; (8) LoRa antenna 868-915 MHz; (9) DC Voltage sensor 0-25V; (10) Anemometer; (11) BH1750FVI illuminance sensor and (12) LEDS fault flags.

Preliminary tests were performed on the protoboard (test board for electronic circuits) to determine the interconnection between sensors and WiFi Lora 32 V2 board. According to [29], the great advantage of using test boards for electronic circuits design is the ease of connecting the components, as it does not require soldering. Through these tests, the best communication architecture between the sensors and the WiFi Lora 32 V2 board was defined, since this board has a synchronous serial interconnect SPI (Serial Peripheral Interface) and I²C (Inter Integrated Circuit). The use of serial communication protocols in embedded systems is related to the low number of pins used and the ability to implement a simple network configuration between peripherals and microcontroller [21].

According to [9], the I²C protocol is a serial bus multimaster, which can have multiple masters, and it is used to connect low-speed peripherals using only two transmission lines (Fig. 2): one is the SDA (Serial Data Line) responsible for data transmitting bidirectionally, and another is the SCL (Serial Clock Line) having the clock generated by the master.

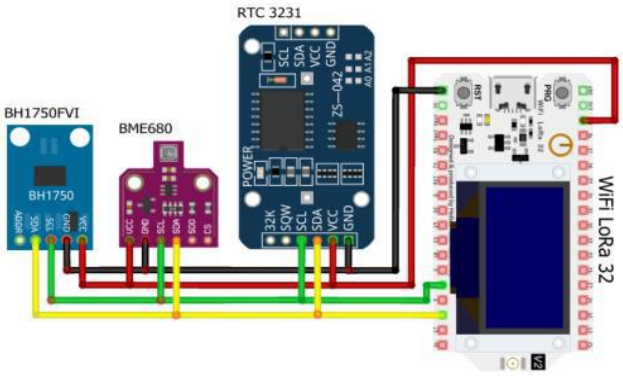

Fig. 2 I²C serial bus of the DAS_T system. Graphic circuit using Fritzing software version 0.9.10.

SPI is also a synchronous, but high-speed serial communication bus created by Motorola and used to connect CPU control devices or peripherals. The communication bus consists of four transmission lines (Fig. 3): SCLK (Serial Clock), MOSI (Master Output and Slave Input), MISO (Master Input and Slave Output) and SS (Slave Selection). The communication configuration is based on the master and slave architecture, with the device working in master mode, usually a microcontroller, which is responsible for the clock pulses that synchronize the data transmission [31].

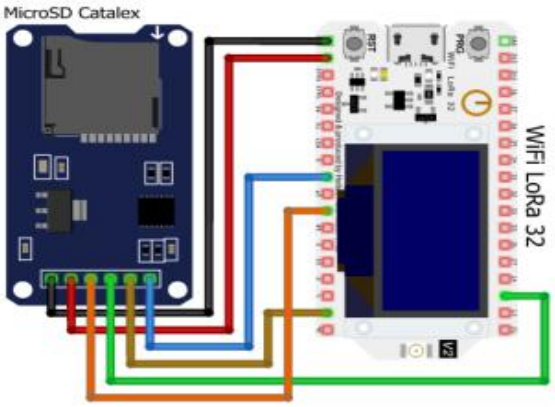

Fig. 3 DAS_T system SPI serial bus. Graphic circuit using Fritzing software version 0.9.10.

After defined the SPI e I²C communication protocols, the final circuit board was prototyped with EasyEDA software, which is an online electronic circuit simulator. Then prototyping, the heat transfer process was carried out on the double-sided copperplate.

Four LEDs were installed in DAS_T to report sensors failures, as shown in Fig. 4. This improvement was necessary for a quick visualizations of sensors information.

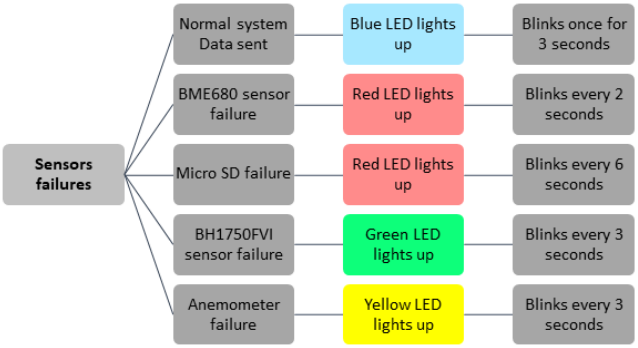

Fig. 4 Visual faults information in DAS_T.

3. Sensors laboratory tests and peripherals

As the objective of the study is to provide a low-cost microclimate monitoring system with reliable information, all sensors incorporated into the DAS_T were submitted to laboratory tests to validate its measurements. For each sensor, a system was made on a protoboard and specific analyzes were conducted. The laboratory tests were based on the comparison between the results of sensors and Reference equipment (traditional measurement equipment). Technical data provided by manufacturers of both sensors and reference equipment were also used. The Arduino IDE (Arduino Integrated Development Environment) platform was used to visualize and store the measurements, which allows the development and writing of codes directly on the microcontroller, and it is a free software. Through this platform, the codes were uploaded onto the board and the measurements of each sensor connected to the board were visualized on its serial monitor.

Some libraries for the correct functioning of the Arduino IDE platform were installed due to the use of WiFi LoRa 32 V2 board. These libraries are available from the GitHub repository, which is a cloud-based service that hosts a version control system called Git. This service allows developers to collaborate and suggest changes in shared projects, being a very popular social networking platform for coding and project hosting service [16].

Sensors specification tests were carried out after each sensor's programming codes were developed and tested. In the specification tests, it was verified that the sensors behave according to the manufacturers' specifications, and later, its results were validated by comparing with the measurements of the reference equipment.

3.1. Sensor CJMCU BME680

BME680 is a four-in-one digital sensor with gas, humidity, pressure and temperature measurement, widely used in low-cost automation projects. The sensor module is housed in an extremely compact metal cover LGA package measuring just 3.0 × 3.0mm² with a maximum height of 1.00mm. Due to its small size and low-power consumption, it allows integration into battery-powered devices [24]. The communication between the WiFi LoRa 32 V2 board and the BME680 was performed through the I²C protocol using pins 4 and 15 (SDA and SCL) of the board, along with other sensors through the multimaster serial bus (Fig. 3).

For temperature values validation, a drying oven (model 400/2ND-300, Nova Ethics) adapted with temperature and refrigeration control (Full Gauge model MT-512E) was used as reference equipment. This adaptation was necessary to ensure that the temperature values measured by the sensor were within the values specified by the manufacturer (Table I). The tests were performed with temperature ranging from 25 °C to 45 °C, with an increase of 5 °C. For each measurement, a stabilization time of 5 minutes was used, totaling 744 samples or measurements.

For humidity data, a Multifunction equipment (HOMIS 4 x 1 model 425A) was used as a reference equipment to verify the relative humidity in the air. The tests were performed during 6 days and 5 measurements were taken during each day at different times, totaling 30 measurements.

Table I : Temperature and humidity parameter specification

Parameter	Details
Model	BME 680
Supply voltage Range	VDD 1.71 V to 3.6 V/ VDDIO 1.2 V to 3.6V
Digital interface	I²C (up to 3.4 MHz) / SPI (up to 10 MHz)
Supply Current[a]	2.1µA
Temperature parameter specification	
Operating temperature range	-40 to 85 °C
Absolute accuracy (25°C)	± 0.5 °C
Absolute accuracy (range of 0°C to 65°C)	± 1.0 °C
Humidity parameter specification	
Operating humidity range	0 to 100 % r.H
20–80 % r.H., 25 °C,	± 3 % r.H

including hysteresis		
Hysteresis[b]	10 to 90 (10 % r.H., 25°C)	± 1.5 % r.H

[a]1Hz forced mode, temperature and humidity measurement, and 1A (power supply) if only temperature measurement. bFor hysteresis measurement the sequence 0→10→30→50→70→50→30→10% r.H. is used.

3.2. Sensor BH 1750FVI

The BH1750FVI Light Sensor is capable of measuring the luminous flux per unit area (LUX), with the ability to perform light intensity measurements in the range from 1 to 65535 lx, uses the I²C communication protocol making it o extremely easy to use with microcontrollers [27].

The communication between this sensor and the WiFi LoRa 32 V2 board was performed through I²C using pin 4 and 15 (SDA and SCL) of board (Fig. 3). For illuminance measurement without external interference, a fully insulated box was assembled with internal lighting and light intensity control. This control was performed with a voltage control circuit equipped with two 12 Volt sources and with voltage modulation through a potentiometer. The Multifunction equipment (HOMIS 4 x 1 model 425A) was used as reference equipment to verify the environment illuminance. Led strips and two sensors were fixed inside the box, one being the reference equipment and the other, the analysis sensor. Subsequently, to obtain higher illuminance values, a shelving system was made with two Led luminaires of 24W each. Measurements were performed with a stabilization interval of 2 minutes. At the end of each measurement, the sensors were covered to always start it at zero.

3.3. Anemometer

The wind speed sensor used is a cup-type anemometer that measures speed through electrical pulses of 3.3 volts for each complete revolution, and its operation is based on a red switch (magnetic key). The red switch is activated by passing a magnet fixed to the anemometer body, and according to the data sheet, if the wind speed is 2.4 km/h, the activation occurs once per second [3].

The anemometer is connected to pins 32 and GND of the LoRa 32 V2 WiFi board. Moreover, the pin interruption method is used in the microcontroller programming to monitor electrical pulses of 3.3 Volts for each complete turn.

Based on the study by [14] of wind tunnel calibration of cup anemometers, a wind tunnel was used to validate the anemometer results, since it was possible to vary the wind speed to perform the measurements. As reference equipment, a portable digital thermo-hygro-anemometer-luxmeter THAL-300 was used fixed close to the anemometer inside the simulator. The values measured by the anemometer were registered by an Arduino IDE platform, with an approximate time of two minutes for each speed step between 0 and 53 km/h. Fifteen speed steps were performed and 73 values were measured in each step, totaling 1095 speed measurements. To monitor the speed in Km/h, a mathematical expression was implemented via code to obtain the correct measurements of the speed in Km/h.

3.4. DC voltage sensor

The system battery voltage was monitored by a DC voltage sensor, which works on the principle of voltage dividers. This sensor can be used in 5 Volts and 3.3 Volts microcontrollers and it is also capable of measuring voltages up to 25V and 16.5V. The sensor was adapted below the microcontroller to optimize the space on the circuit board and it was connected to the input of LoRa 32 WiFi board, monitoring the 6V battery voltage. A digital multimeter (HM-2400 from Hikari) was used as reference equipment, connected in parallel to the input of LoRa 32 WiFi board to measure the battery voltage. Measurements were taken every 15 seconds, totaling 30 samples.

3.5. Photovoltaic solar panel

A solar panel (KOMAES model KM-10) was used to supply power to the system and charge the battery, making an autonomous system in energy supply. According to [17], the solar panel has 36 polycrystalline silicon cells with a maximum power of 10W, the maximum voltage is 17.56V and a maximum current of 0.6A. Therefore, the daily energy generation, according to the solar panel supplier, is approximately 3.0 Ah/day (data based on the national average of 5 hours of insolation 1000W/m² of irradiation) as shown in Table II.

Table II: Technical specifications solar panel komaes km10 (10wp).

Parameter	Details
Maximum Power (Pm):	10 W
Tolerance:	-5%/+5%
Maximum Power Voltage (Vm):	17.56 V
Maximum Power Current (Im):	0.60 A
Open Circuit Voltage (Voc):	21.52 V
Short-Circuit Current (Isc):	0.66 A
Maximum System Voltage:	50 V
Panel Efficiency:	10,8%

Power Temperature Coefficient (Pm):	-0,45 %/°C
Current Temperature Coefficient (Isc):	0,06 A/°C
Voltage Temperature Coefficient (Voc):	-0,37 V/°C
Nominal Cell Operating Temperature (TNOC/NOCT):	46±2°C

*Standard STC/CPT Test Conditions: Irradiation of 1,000 W/m², Air Mass Spectrum 1.5 and Cell Temperature of 25°C.

3.6. Photovoltaic solar controller

According to [25], charge controllers aim to protect the battery against excessive charges and discharges, thus increasing its useful life. The charge controller is considered indispensable in photovoltaic systems and its use allows the disconnection of loads in a low state of battery charge and a greater level of protection against an excessive increase in consumption.

The controller used in this study was the DHS-3S/5S/10S model manufactured by CHINALAND, which is equipped with a microcontroller that controls the system to avoid overload, excessive release of battery charges in low state, electronic short circuit and reverse battery connection. Three operating modes can be selected: normally open mode, full load control mode and load control plus timing mode. Considering the operational definition of the projected microclimate system, the normally open mode was chosen. In this mode, the entire electrical supply to the system is carried out by the solar panel and regulated by the controller (Fig. 5). When there is not enough power generation to supply the system, the controller starts to supply power through the battery.

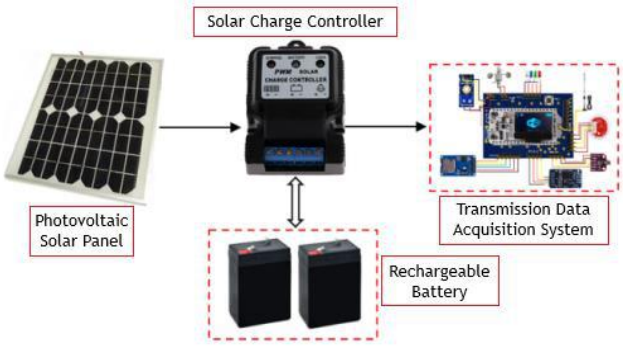

Fig. 5 Load controller system architecture.

3.7. Rechargeable battery

Two batteries were used to supply electricity for the microclimate monitoring system when weather conditions were not favorable for electricity generation by the solar panel. These batteries are one of the Unipower Brand model UP645SEG and other of the Kaise model KB640 (Table III).

Table III: Unipower battery model up1250 parameters and specifications.

PARAMETER	Details Unipower	Details Kaise
Model	UP645SEG	KB640
Supply voltage	DC 6V	DC 6V
Capacity (C10)[a]	3.86 Ah	3.77 Ah
Capacity (C20)[a]	4.5 Ah	4.0 Ah
Floating use	6.75 - 6.9V	6.75 - 6.9V
Cycle use	7.05 – 7.20V	7.20 – 7.50V
Maximum recharge current	1.2A	1.2A
Parameter	Details Unipower	Details Kaise
Model	UP645SEG	KB640
Supply voltage	DC 6V	DC 6V
Capacity (C10)[a]	3.86 Ah	3.77 Ah
Capacity (C20)[a]	4.5 Ah	4.0 Ah

*Standard STC/CPT Test Conditions: Irradiation of 1,000 W/m², Air Mass Spectrum 1.5 and Cell Temperature of 25°C.

The WiFi LoRa 32 V2 board was tested in two operating modes, active and hibernation, with the objective of reduce DAS_T system consumption and to obtain better batteries performance during the microclimate monitoring system operation. The LoRa 32 V2 WiFi board can be programmed to remain in hibernation mode, while the data is not transmitted, and it can be woken up by external signals or by time programming [11].

The time required for the battery to power the microcontroller operation was calculated using a digital multimeter (Hikari HM-2400) connected to the system as an ammeter. This equipment performed electrical current measurements during five system operation cycles, as follows:

- Active mode: complete operation process, which varies according to the number of

measurements/samples requested from the system. For the test, 100 samples were requested, totaling approximately, one minute and fifty seconds. After this time, the microcontroller stops processing sensor information, but remains active;

- Hibernation mode: power-saving state, which continue for approximately 5 minutes. After this time, the microcontroller starts in active mode and remains in this mode according to the number of samples requested. In this test, a total of 100 samples were requested from the system.

3.8. Module real-time Clock Ds3231

The DS3231 real-time Clock (RTC) is a high-precision clock, which maintains the synchronization of date and time information. RTC also has a 3V Lithium battery that maintains accurate information when the device's main power is interrupted [19].

The communication between WiFi LoRa 32 V2 board and the RTC was done by the I²C (Inter-Integrated Circuit) protocol, using pins 4 and 15 (SDA and SCL), as shown in Fig. 3. Date and time accuracy was verified through a protoboard system composed of the BME680 sensor, which performed temperature and relative humidity measurements. Each measurement was realized at 20-minutes intervals during 30 days, totaling 2160 measurements. The Arduino IDE platform was used as a reference for time validation. Thus, through the serial monitor screen, the time informed by RTC was shown and also the time recorded by Arduino IDE.

3.9. MicroSD card module

Data logger is used to record data over time using sensors or external instruments [20]. However, occasionally, it is necessary to store a large amount of data measured by sensors and other information, and NAND Flash memory is an important tool for this purpose, since EEPROM memory of microcontrollers is limited in data storage size. NAND Flash memory in portable version are SD cards, whose storage size and file systems vary, FAT16 or FAT32 [2].

The Catalex MicroSD Card was used in this study, allowing measurements and writing on a MicroSD card that is easy to connect to the LoRa 32 V2 WiFi card, and can be powered by 3.3 Volts or 5 Volts. The interconnection of the MicroSD card module with the LoRa 32 V2 WiFi card is performed through the SPI (serial peripheral interface) communication protocol, and it is connected to the SPI hardware pins (Fig. 4). Its interconnection to the board would be through pins 5, 19, 27, 18 (SCK, MISO, MOSI, SS), but after studies it was found that it uses these pins for board control functions, therefore, it must not be used for other purposes. Therefore, it was necessary to program a second class of SPI communication enabling pins 17, 23, 12, 22 (SCK, MISO, MOSI, SS) to connect the MicroSD card module and obtain its correct operation.

4. Receiving system

The receiving data acquisition system (DAS_R) was responsible for receiving, storing and connecting to the internet for microclimatic monitoring sent by the DAS_T (Transmitter Data Acquisition System). The architecture of DAS_R is illustrated by Fig. 6.

Fig. 6 Structure system of the DAS_R. (1) LoRa 32 V2 WiFi board; (2) MicroSD module card; (3) Antenna LoRa 868 MHz - 915 MHz and (4) 5V power supply.

ThingSpeak platform was used to access the data received by DAS_T from anywhere with an internet connection. This platform is an IoT service, which allows visualization, analysis and upload of data sent from cloud-connected devices [1]. In all interaction of the systems for samples/measurements collection, these data were visualized on the LCD display of LoRa 32 V2 WiFi board.

5. Statistical analysis

Were Descriptive statistic tests and frequency tests applied to exploratory data analysis. The statistics test were used to verify to verify if the data provided are sufficient to accept as true the hypothesis that the average of sensors measurements were compatible with those of the reference equipments, in significance level of 5%. For data analysis, the Student's T test was applied for the independent variables, and simple linear regression (ANOVA) was used to correct the variables which showed significance difference in its average. The hypothesis tests were used to verify the necessity of adjustment in the sensors results by the application of a polynomial algorithm and, compare them with those of the reference equipment [26].

III. RESULTS AND DISCUSSION

3.1 Measurement tests and validation of sensors and peripherals

First, the statistical result of the comparison of means, standard deviation and error of the sample means were used to verify possible discrepancies between the measurements performed by the reference equipment and the test sensors (Table IV). It was observed that the five is sensors studied did not differ significantly from the measurements of the reference equipment, namely: Temperature (34.68; 34.83), Humidity (44,20; 44,20), Illuminance (3896.71; 3872.49).

Table IV: Average standard deviation of reference equipment and test sensors.

Parameters	Samples	µEq.P	µSensor
Temperature	744	34.68 ± 6.92	34.83 ± 6.77
Humidity	23	44.20 ± 15.60	44.20 ± 15.90
Illuminance	124	3896.71 ± 5619	3872.49 ± 5788
Anemometer	1184	31.32 ± 13.14	34.75 ± 17.10
Voltage	30	7.36 ± 0.09	6.24 ± 0.06

* µEq.P Average value of the measurements of the reference equipment.

To statistically verify the equality or not of the averages of the sensor readings, the Student's T test was applied, which according to Figure 7, the sensors responsible for the temperature variables (°C) (p = 0.68), relative humidity (%) (p = 0.99) and illuminance (Lux) (p = 0.97), statistically resulted in the acceptance of the null hypothesis that their means did not differ significantly. Thus, the null hypothesis was rejected for the anemometer (p<0.05) and voltage (p<0.05) sensors, since their means diverged significantly.

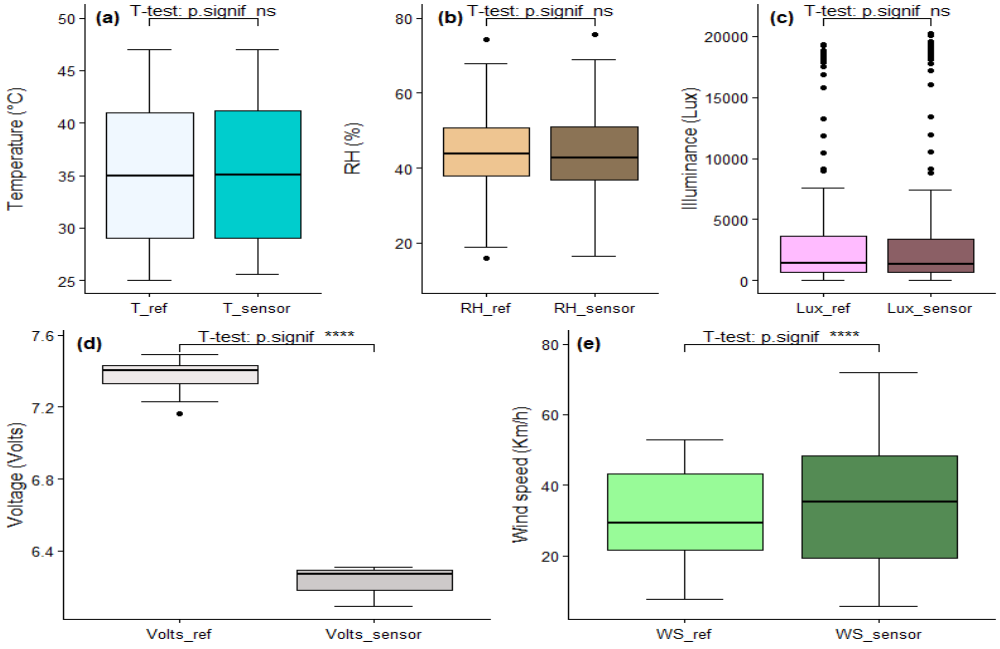

Fig. 7 Box plot showing the differences between reference equipment and sensors. Whiskers and box bands denote quartiles. Comparison using Student's t test for independent samples showed that: (a) Temperature °C (ns); (b) RH % (ns); (c) Illumination (Lux) (ns); (d) Wind Speed (Km/h)(****) and (e) Voltage sensor (Volts)(****).

Regarding the results of the Student's T test, in which two of the five sensors showed divergence between the means, an analysis of variance (ANOVA) was performed on all sensors (Fig. 8). This test evaluates the percentage of variation of the response variable, which is explained by a linear model, and reduces the measurement error of the sensors under analysis in relation to the reference equipment.

The results showed that the anemometer sensor (Fig. 8d) and the battery voltage sensor (Fig. 8e) showed a small

difference in relation to the reference equipment, requiring the implementation (via code in the microcontroller) of the corresponding equation obtained through analysis of variance (ANOVA), to correct the readings and increase the reliability of the measurements.

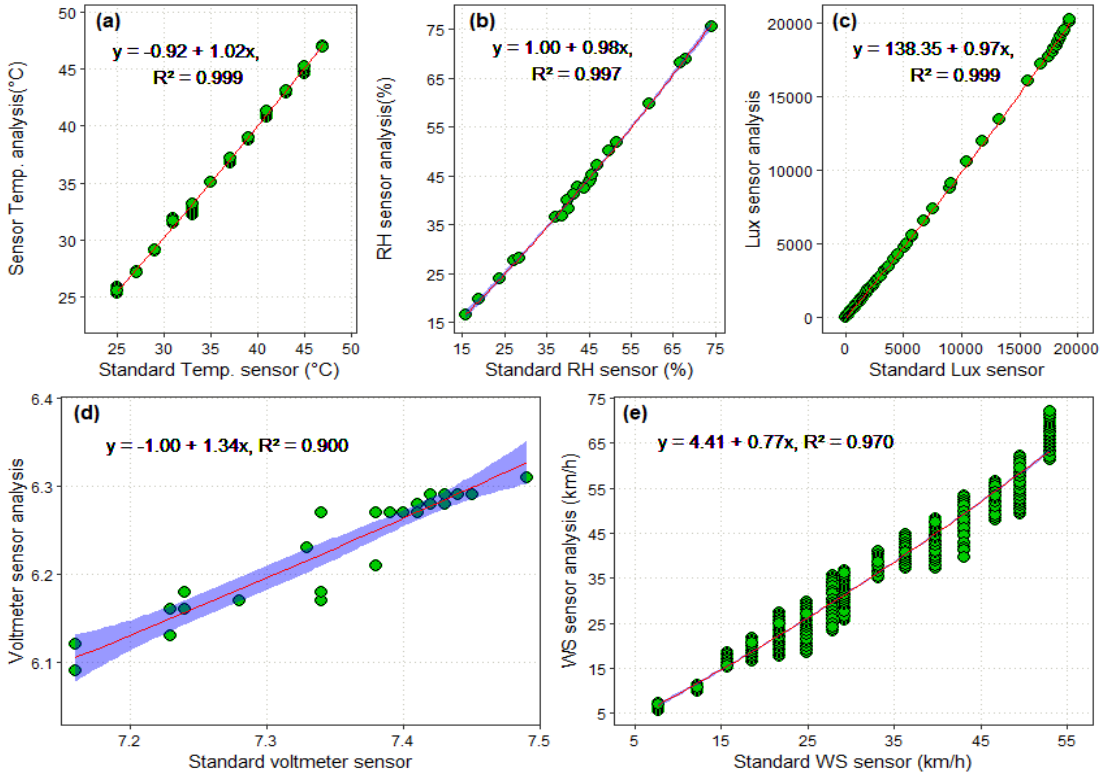

Fig. 8 Results of simple linear regression analysis applied between measurements of the reference equipment and the sensors: (a) Temp. (Temperature °C); (b) RH (Relative Humidity %); (c) Illumination (Lux); (d) WS (Wind Speed Km/h) and (e) Voltage sensor (Volts).

Regarding Module real-time Clock Ds3231, the objective was to verify if the time in hours and minutes were being recorded correctly by the system, therefore, a period of 30 days was analyzed to have a sufficient database for analysis.

After the 30-day test period, 2036 measurements were obtained, with an average time of twenty-one minutes and twenty-four seconds. The reference time is 20 minutes, which is the time required for the system to perform the following tasks: hibernate; collect 100 measurements and calculate its average; save a copy on the SD card; send the data to the receiving system and sleep again. The Arduino IDE platform was used to compare the time measured by the sensor and the time recorded by the system, showing a difference of only twenty-one seconds of delay.

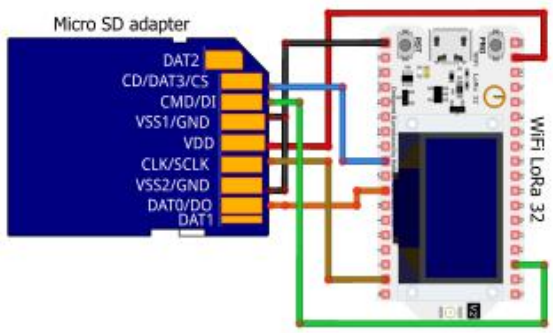

Fig. 9 Fig. 9. Connecting the Micro SD card adapter directly. Graphic circuit using Fritzing software version 0.9.10.

The individual functioning of each element (sensors, registers, among others) from the system was evaluate with the purpose of reducing the energy consumption of batteries. The microSD card has an operating voltage of 3.3 Volts compatible with LoRa 32 V2 WiFi card from Heltec, so the use of the Catalex MicroSD Card module

would not be necessary. However, as the system is powered by battery and, predicting the worst scenario for energy generation by the solar panel KOMAES to recharge it, the consumption of the Catalex module was evaluated. A direct interconnection was made at the card interface with the microcontroller through the MicroSD adapter (Fig. 9) to evaluate wether there is a significant reduction in the system consumption.

Tests were carried out with the Hikari's HM-2400 Digital Multimeter connected to the system as an ammeter, and the current measurement was performed with the system working with the Catalex module; and with the direct connection on the MicroSD adapter. The consumption difference was approximately 4.3 mA (milliampere), which is a minor difference and does not include battery performance. Therefore, the Catalex module was used for the DAS_R and the DAS_T systems (Fig. 1 and Fig. 6).

The communication between the DAS_R/DAS_T system is the most important point of this study, as it guarantees that all information collected will be sent and received by the system. So, tests were conducted at medium distance to evaluate the data sending and receiving. Thus, the original antenna supplied with the LoRa 32 V2 WiFi card was tested to verify its range. Through Google Maps platform, it was observed that a distance of 1 km was reached, and all information was sent and received by the system without interruptions (Fig. 10).

Fig. 10 Communication distance between systems with original antenna and TX900 antenna.

Considering that the developed system would be placed where DAS_T internet networks are not available, an attempt was made to increase the communication distance. Thus, the original antenna was replaced by one with greater range capacity. The Omnidirectional antenna, model ZIISOR TX900-XPL-200, with 23cm was acquired (Table V). In connecting the new antenna to the board, a 15cm pigtail cable was used, since in smaller cables, the loss in db (decibels) is also lower. After the tests, a greater range of approximately 3.5 km was obtained without loss of information (Fig. 10).

Table V: Technical specification tx900-xpl-200

Parameter	Data	Parameter	Data
Frequency	900MHz	Height	260mm
Band	860-960MHz	Base Diameter	30mm
Gain	4 dBi	Total Weight	28 g
SWR	≤1.5	Feeder Length	2m
Polarization	Vertical	Feeder Material	RG174
Radiation Direction	Omnidirectional	Connector	SMA Male

For the purpose of reducing the size of the DAS_T, system was assembled with an 8.4V/28,800mAh Li-ion rechargeable battery pack provided by J.W.S. After several tests, it was observed that this battery model did not support the required work regime, discharging completely in the periods when it was not being recharged by the KOMAES solar panel. Consequently, the new batteries of Unipower model UP645SEG and Kaise model KB640 (Fig. 11) were adopted as the power supply.

As the batteries used in the DAS_T system was changed, it was necessary to place it in a separate compartment due to its size, being adapted in a box with an IP66 degree of protection, without contamination from external agents, such as rainwater. A charge controller model DHS-3S/5S/10S was also installed inside the same compartment (Fig. 11), controlling the voltage and current supplied to the battery, automatically.

Fig. 11 Mounting the system battery and charge controller.

3.2 Final project

DAS_T/DAS_R systems were placed in polyvinyl chloride (PVC) tubes, in order to be protected from external agents. This type of material is affordable, versatile and low-cost. DAS_R was structured to be indoors, such as offices, laboratories, among others. Fig. 12 shows the DAS-R, with LCD display, 5 Volts power supply with input, local antenna connection, MicroSD card access and Wifi access to send data to the cloud.

Fig. 12 Final structure of PVC DAS_R.

When DAS_R is connected to the Internet network, the recorded data was sent to the ThingSpeak platform, which is used as a support for monitoring and storing data. Through the ThingView App it is possible to access the data by via mobile device (Fig. 13).

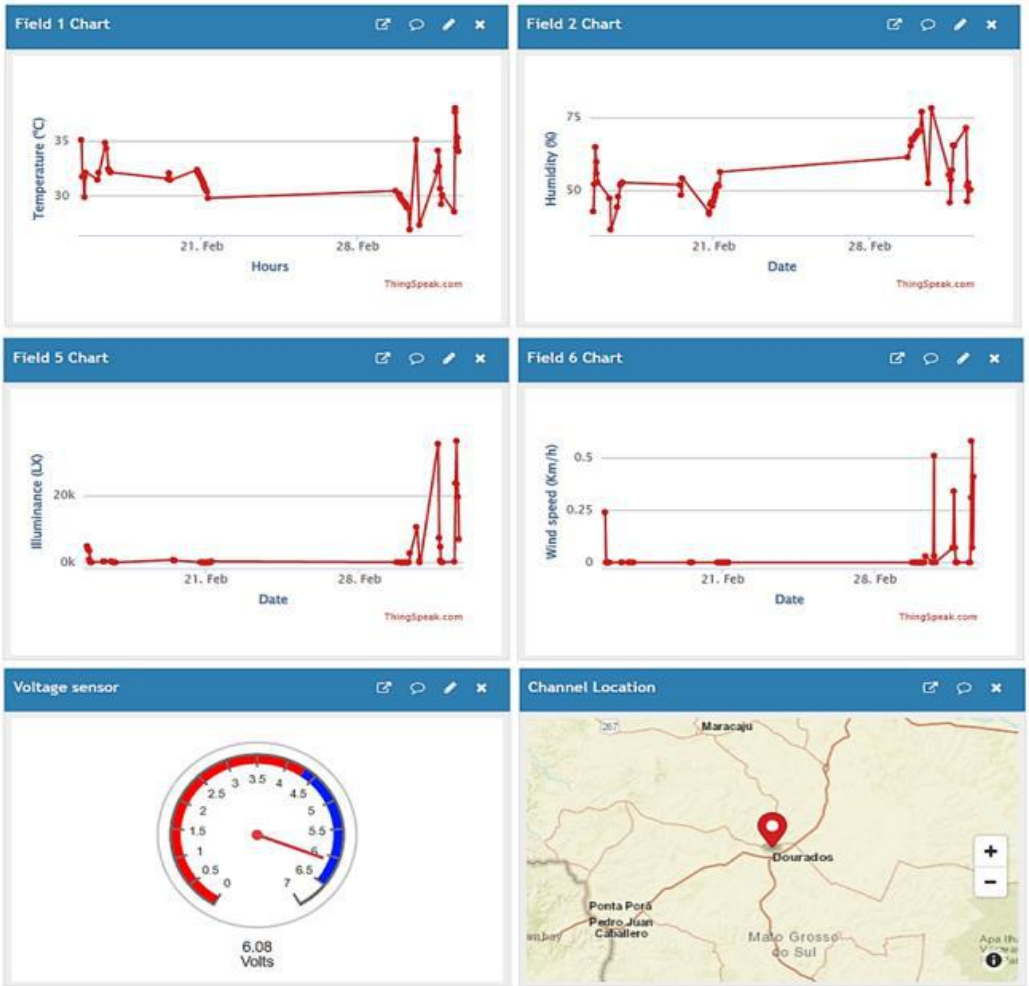

Fig. 13 Microclimatic data recording on the ThingSpeak platform.

The DAS_T (Fig. 14) is composed of the printed circuit board, all sensors, the RTC module, the MicroSD card module, the battery power input and, in a separated a structure, the solar board KOMAES and the system battery.

Fig. 14 Final structure system DAS_T.

1. Total cost of systems: DAS_T and DAS_R

Table VI shows the cost of each component of the microclimate monitoring system, also including the materials used to house the two systems. The total cost of DAS_T and DAS_R was US$ 283.56 (values referring to the year of this work). Compared with conventional meteorological systems, whose values range from US$ 527.00 to $3.000.00, the microclimate monitoring system exhibited in this study presented a lower value, in addition to presenting radiofrequency communication. The conventional meteorological systems communicate by connecting to a Wi-Fi or cellular network, so, it cannot be used to support real-time microclimate monitoring in places where internet is unavailable.

Table VI: Cost of final project – DAS_T and DAS_R.

Components	Manufacturer	Quantity	Cost US$
WiFi LoRa 32 (V2.1)	HELTEC AUTOMATION(TM)	2	81.28
BME680 Temperature Humidity Sensor	CJMCU	1	19.00
Illuminance Sensor BH1750FVI (V1.0)	KEYESTUDIO	1	7.97
Voltage sensor (VCC<25V)	MINGYUANDINGYE	1	5.41
Wind sensor	ARGENT DATA SYSTEMS	1	23.91
RTC module AT24C32 DS3231	MINGYUANDINGYE	1	6.49
MicroSd Card Adapter	CATALEX	2	9.46
Micro SD Memory Card 16Gb	SANDISK	2	18.29
Antenna Lora wifi 868 mhz - model TX900-XPL-200	ZIISOR	2	32.90
Solar power control – model DHS-5S-6V12V10A	CHINALAND	1	12.01
Photovoltaic Solar Panel - model KM-10	KOMAES	1	26.83
Rechargeable battery model UP1250 (6v4.5Ah)	UNIPOWER	1	15.81
Rechargeable battery model KB640 (6v4.0Ah)	KAISE	1	12.22
pvc tube cap 100mm	TIGRE	4	9.95
PVC pipe diameter 100mm	TIGRE	1/2	12.18
Total cost			$283.56

IV. CONCLUSION

This work presented as a guiding parameter, which is the validation of a long-distance and low-cost microclimate monitoring system, with reliable information. The validation tests of the sensors were important to prove that the direct use, or not, of these sensors could faithfully measure all the microclimate variables studied in this work. Although the results of the validation test were satisfactory, a statistical comparison was applied between the measurements of sensors and reference equipment. This comparison showed that all the sensors used measured the studied parameters with feasibility, with the exception of two sensors, wind speed and battery voltage. Therefore, the developed system could be used in microclimate monitoring experiments after the calibration of these two sensors through the linear models proposed in this work.

Finally, the proposed low-cost system presented positive results in comparison to the systems with higher added value for measurements of temperature, relative air humidity, illuminance (lx) and wind speed. In addition, the present work showed the development of systems in which there is a need for environmental monitoring where there is no access to the Wi-Fi network, since communication

between receiver and transmitter was maintained for a distance of approximately 3.5 km. The system can also be incorporated with other sensors, such as for monitoring carbon dioxide (CO2), as the DAS_T system is already capable of inserting the sensor, remaining the same for future works. incorporated with other sensors, such as for monitoring carbon dioxide (CO2), as the DAS_T system is already capable of inserting the sensor, remaining the same for future works.

REFERENCES

[1] Aba, E. N., Olugboji, O. A., Nasir, A., Olutoye, M. A., & Adedipe, O. (2021). Petroleum pipeline monitoring using an internet of things (IoT) platform. SN Applied Sciences, 3(2). https://doi.org/10.1007/s42452-021-04225-z

[2] Aiea, V. M. (2019). Interfacing Catalex Micro SD Card Module with Arduino. 21/02/2019. Disponível em: https://www.vishnumaiea.in/projects/hardware/interfacing-catalex-micro-sd-card-module. Acesso em: 10 jan. 2022.

[3] Argent Data Systems. Disponível em: https://www.argentdata.com/catalog/product_info.php?products_id=175. Acesso em: 25 jan. 2022.

[4] Bafdal, N., & Ardiansah, I. (2021). Application of Internet of Things in Smart Greenhouse Microclimate Management for Tomato Growth. International Journal on Advanced Science, Engineering and Information Technology, 11(2), 427–432. https://doi.org/10.18517/ijaseit.11.2.13638

[5] Bringmann, D. R., Gamba, T. D. O., Carolina, M., & Gullo, R. (n.d.). A sustentabilidade ambiental, econômica e social nas clínicas e consultórios odontológicos: uma revisão sistemática. Disponível em: https://preprints.scielo.org/index.php/scielo/preprint/view/1663. Acesso em: 15 fev. 2022. https://doi.org/10.3390/s20216225

[6] Carvalho, J. M., Gurjão, E., & Veloso, L. R. (2015). Introdução a Análise de Sinais e Sistemas. In Elsevier (Ed.), Elsevier (1st ed.). 2015.

[7] Catargiu, G., Dulf, E. H., & Miclea, L. C. (2020). Connected bike-smart IoT-based cycling training solution. Sensors (Switzerland), 20(5). https://doi.org/10.3390/s20051473

[8] DeweSoft. (2020). O que é Aquisição de Dados - DAQ ou DAS? Disponível em: <https://dewesoft.com/br/aquisicao-de-dados/o-que-e>. Acesso em: 20 jan. 2022.

[9] Do Nascimento, G. A. M., Neto, M. M. L., & Da Silva, W. B. (2021). Uma Aplicação Didática do Protocolo I²C em Sistemas de Comunicação / A Didactic Application of the I²C Protocol in Communication Systems. Brazilian Journal of Development, 7(10), 94837–94853. https://doi.org/10.34117/bjdv7n10-001

[10] Emilio, M. D. P. (2013). Smart Data Acquisition System. In Data Acquisition Systems (pp. 123–131). Springer New York. https://doi.org/10.1007/978-1-4614-4214-1_6

[11] Espressif Systems (2021). ESP32 Series Datasheet. In Espressif Systems. Disponível em:https://www.espressif.com/sites/default/files/documentation/esp32_datasheet_en.pdf. Acesso em: 10 jan. 2022.

[12] González, E., Casanova-Chafer, J., Romero, A., Vilanova, X., Mitrovics, J., & Llobet, E. (2020). Lora sensor network development for air quality monitoring or detecting gas leakage events. Sensors (Switzerland), 20(21), 1–21. https://doi.org/10.3390/s20216225

[13] Hajjaji, Y., Boulila, W., Farah, I. R., Romdhani, I., & Hussain, A. (2021). Big data and IoT-based applications in smart environments: A systematic review. Computer Science Review, 39, 100318. https://doi.org/10.1016/j.cosrev.2020.100318

[14] Hansen, O. F., Hansen, S. O., & Kristensen, L. (2012). Wind Tunnel Calibration of Cup Anemometers. AWEA Wind Power Conference 2012, 1–22.

[15] Heltec Automation. WiFi LoRa 32 (V2). Disponível em: <https://heltec.org/project/wifi-lora-32/>. Acesso em: 10 fev. 2022.

[16] Hu, Y., Zhang, J., Bai, X., Yu, S., & Yang, Z. (2016). Influence analysis of Github repositories. SpringerPlus, 5(1). https://doi.org/10.1186/s40064-016-2897-7

[17] Komaes. Komaes Solar - Polycrystalline Solar Modules: Off-Grid Modules. Disponível em: http://www.KOMAES-solar.com/products-1.asp. Acesso em: 06 fev. 2022.

[18] Magrani, E. (2018). A internet das coisas (FGV (ed.). 2018.

[19] Maxim Integrated. (2015). Extremely Accurate I 2 C-Integrated RTC DS3231 (pp. 1–19). Disponível em: <http://datasheets.maximintegrated.com/en/ds/DS3231.pdf>. Acesso em: 10 jan. 2021.

[20] Méndez-Barroso, L. A., Rivas-Márquez, J. A., Sosa-Tinoco, I., & Robles-Morúa, A. (2020). Design and implementation of a low-cost multiparameter probe to evaluate the temporal variations of water quality conditions on an estuarine lagoon system. Environmental Monitoring and Assessment, 192(11). https://doi.org/10.1007/s10661-020-08677-5

[21] Murali, A., Kakarla, H. K., & Anitha Priyadarshini, G. M. (2021). Improved design debugging architecture using low power serial communication protocols for signal processing applications. International Journal of Speech Technology, 24(2), 291–302. https://doi.org/10.1007/s10772-020-09784-x

[22] Oliveira, L. P. M. de, Silva, F. D. dos S., Costa, R. L., Rocha Júnior, R. L. da, Gomes, H. B., Pereira, M. P. S., Monteiro, L. A., & Silva, V. de P. R. da. (2020). Impacto das Mudanças Climáticas na Produtividade da Cana de Açúcar em Maceió. Revista Brasileira de Meteorologia, 35(spe), 969–980. https://doi.org/10.1590/0102-77863550107

[23] Oliveira, M. M., Esteves, P. M. da S. V., Baía, S. R. D., Dantas, N. da S., & Silva, V. F. (2020). Análise da produção científica internacional sobre mudanças climáticas e poluição do ar. Research, Society and Development, 9(10), e1609108314. https://doi.org/10.33448/rsd-v9i10.8314

[24] Penkov, S., & Taneva, A. (2021). Chat programs in the frame of control system. IFAC-PapersOnLine, 54(13), 52–56. https://doi.org/10.1016/j.ifacol.2021.10.417

[25] Pinho, J.T. et al. Manual de engenharia para sistemas fotovoltaicos. Rio de Janeiro, v. 1, p. 47-499, 2014.

[26] Sharpe, N. R., Veaux, R. D. De, & Velleman, P. F. (2011). Estatística Aplicada Administração, Economia e Negócios (Grupo A (ed.); 1st ed.).

[27] Silveira, V. B., Dal Pai, A., & Dal Pai, E. (2021). Avaliação de desempenho do sensor BH1750FVI (baixo custo) na medida da radiação solar global. Research, Society and Development, 10(14), e170101421779. https://doi.org/10.33448/rsd-v10i14.21779

[28] Simarangkir, M. S. H.; Suryanto, A. Prototype Pengunci Pintu Otomatis Menggunakan Rfid (Radio Frequency Identification) Berbasis Mikrokontroler Arduino Uno. Technologic, v. 11, n. 1, 2020. http://doi.org/10.52453/t.v11i1.284

[29] Stevan, S. L.; Silva, R. A. Automação e instrumentação industrial com Arduino: teoria e projetos. Saraiva Educação SA, 2015.

[30] Unesco. (2005). Organização das Nações Unidas para a Educação, a Ciência e a Cultura. Década da educação das Nações Unidas para um desenvolvimento sustentável, 2005-2014: documento final do esquema internacional de implementação. http://unesdoc.unesco.org/images/0013/001399/139937por.pdf

[31] Wang, D., Yan, J., & Qiao, Y. (2021). Design and verification of SPI bus IP core. Journal of Physics: Conference Series, 1971(1). https://doi.org/10.1088/1742-6596/1971/1/012032

[32] Ye, H., Yang, Y., & Zhu, L. (2021). A wireless network detection and control system for intelligent agricultural greenhouses based on NB-IOT technology. Journal of Physics: Conference Series, 1738(1). https://doi.org/10.1088/1742-6596/1738/1/012058